Kinetically stable methylidene complexes ...

… of zirconium and hafnium were prepared through photolysis-induced α-H abstraction from the corresponding complexes with aryloxide and two methyl ligands. In their Communication on page 10913 ff., D. J. Mindiola and co-workers describe their quest for a kinetically more resistant system (structure on top of the compass) by taking advantage of prior systems (old map with drawings), thus finding the target molecule (inside the treasure chest).

Spin-Crossover Nanoparticles

In their Communication on page 10894 ff., L. Salmon, A. Bousseksou et al. determine the Debye temperature for [Fe(pyrazine){Ni(CN)$_4$}] nanoparticles ranging from 2 to 110 nm. The investigations explain the re-appearance of cooperativity in the smallest nanoparticles.

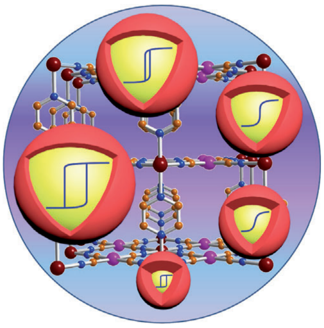

Gas-Phase Reactions

G. N. Khairallah, G. da Silva, and R. A. J. O'Hair describe in their Communication on page 10979 ff. how the addition of an individual salt molecule to an organometallic reagent dramatically enhances its reactivity towards water.

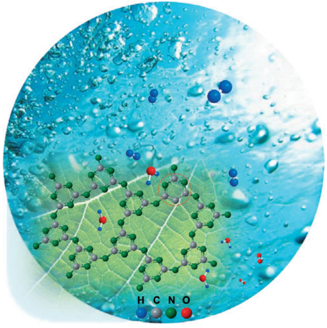

Photocatalysis

A family of crystalline carbon nitrides obtained by supramolecular aggregation and ionic melt polycondensation is shown by K. Takanabe and coworkers in their Communication on page 11001 ff. to give excellent photocatalytic H_2 evolution.

How to contact us:

Editorial Office:
E-mail: angewandte@wiley-vch.de
Fax: (+49) 62 01–606-331
Telephone: (+49) 62 01–606-315

Reprints, E-Prints, Posters, Calendars:
Carmen Leitner
E-mail: chem-reprints@wiley-vch.de
Fax: (+49) 62 01–606-331
Telephone: (+49) 62 01–606-327

Copyright Permission:
Bettina Loycke
E-mail: rights-and-licences@wiley-vch.de
Fax: (+49) 62 01–606-332
Telephone: (+49) 62 01–606-280

Online Open:
Margitta Schmitt, Carmen Leitner
E-mail: angewandte@wiley-vch.de
Fax: (+49) 62 01–606-331
Telephone: (+49) 62 01–606-315

Subscriptions:
www.wileycustomerhelp.com
Fax: (+49) 62 01–606-184
Telephone: 0800 1800536 (Germany only)
+44(0) 1865476721 (all other countries)

Advertising:
Marion Schulz
E-mail: mschulz@wiley-vch.de
jspiess@wiley-vch.de
Fax: (+49) 62 01–606-550
Telephone: (+49) 62 01–606-565

Courier Services:
Boschstrasse 12, 69469 Weinheim

Regular Mail:
Postfach 101161, 69451 Weinheim

Angewandte Chemie International Edition is a journal of the Gesellschaft Deutscher Chemiker (GDCh), the largest chemistry-related scientific society in continental Europe. Information on the various activities and services of the GDCh, for example, cheaper subscription to *Angewandte Chemie International Edition*, as well as applications for membership can be found at **www.gdch.de** or can be requested from GDCh, Postfach 900440, D-60444 Frankfurt am Main, Germany.

GDCh
GESELLSCHAFT
DEUTSCHER CHEMIKER

Service

Author Profile


© Lisa Godfrey

"The most exciting thing about my research is my research team is highly motivated, passionate about science, and rapidly generates interesting results.
My biggest motivation is the thrill of doing more innovative science than we did last week ..."
This and more about Patrick J. Walsh can be found on page 10854.

News


H. Möhwald


K. De Oliveira Vigier


V. Monteil


D. R. Walt

Obituaries

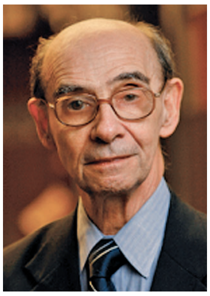

Sheldon G. Shore, Distinguished Professor of Mathematical and Physical Sciences and Charles H. Kimberly Chair of Chemistry at The Ohio State University, died on April 4th, 2014. Shore's research spanned vast areas of the periodic table, but he is probably best known for his pioneering work on boron hydrides, metal carbonyl clusters, and lanthanide/transition-metal systems and their conversion into catalytically active nanoparticles.

Books

Around the World in 18 Elements — David Scott — *reviewed by A. Grohmann* ______ **10857**

Highlights

Synthesis of Liquid Fuels

K. J. P. Schouten, F. Calle-Vallejo,
M. T. M. Koper* ______ **10858 – 10860**

A Step Closer to the Electrochemical Production of Liquid Fuels

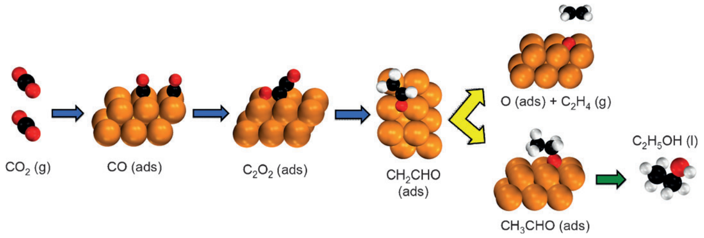

Fueled by success: A nanostructured copper electrocatalyst derived from copper oxide can reduce carbon monoxide to multicarbon oxygenates, including ethanol. This is an important step in the production of liquid fuel by the reduction of CO_2 using electricity from renewable sources.

Arenes

O. Quinonero, C. Bressy,*
X. Bugaut* ______ **10861 – 10863**

Organocatalytic Enantioselective Construction of Polyaromatic Architectures

Aromatics in 3D: Organocatalysis is now reaching beyond the control of stereogenic centers and opens new possibilities for the construction of complex polyaromatic structures with either helical or axial chirality.

Proteomics

J. Muñoz,* A. J. R. Heck* **10864 – 10866**

From the Human Genome to the Human Proteome

A herculean task: Determining the human proteome sets the ultimate challenge in cell biology as it is thought to consist of more than 1 000 000 proteoforms, in contrast to “only” 20 000 protein-coding genes. Two teams of researchers have now proved the translation of 18 000 proteins (and more than 27 000 isoforms) by mass spectrometry. They obtained important information on the extent of protein translation and alternative splicing.

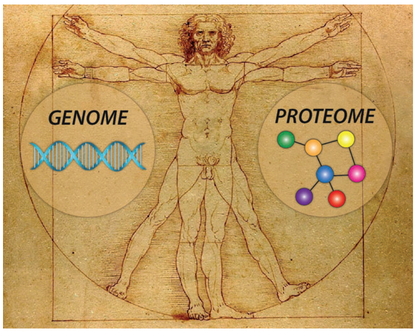

For the USA and Canada:
ANGEWANDTE CHEMIE International Edition (ISSN 1433-7851) is published weekly by Wiley-VCH, PO Box 191161, 69451 Weinheim, Germany. US mailing agent: SPP, PO Box 437, Emigsville, PA 17318. Periodicals postage paid at Emigsville, PA. US POSTMASTER: send address changes to *Angewandte Chemie*, John Wiley & Sons Inc., C/O The Sheridan Press, PO Box 465, Hanover, PA 17331. Annual subscription price for institutions: US$ 11.738/10.206 (valid for print and electronic / print or electronic delivery); for individuals who are personal members of a national chemical society prices are available on request. Postage and handling charges included. All prices are subject to local VAT/sales tax.

Minireviews

Chiral-at-Metal Complexes

L. Gong, L.-A. Chen,
E. Meggers* ________ 10868 – 10874

Asymmetric Catalysis Mediated by the Ligand Sphere of Octahedral Chiral-at-Metal Complexes

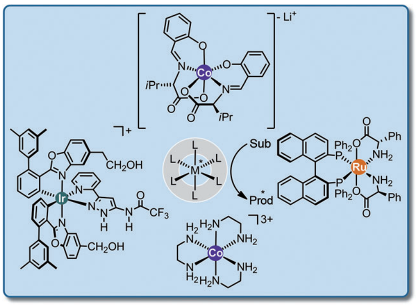

“Organocatalysis” with metal complexes: Inert octahedral metal complexes are an emerging class of catalysts for asymmetric synthesis. In these compounds the globular, rigid nature and stereochemical options of octahedral compounds are exploited. Complexes like those shown promise new opportunities in the field of catalysis.

Reviews

Biofuels

U. Bornscheuer, K. Buchholz,
J. Seibel* ________ 10876 – 10893

Enzymatic Degradation of (Ligno)cellulose

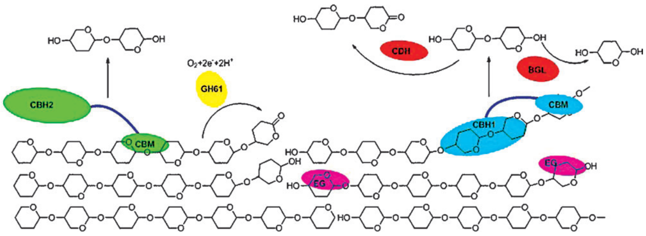

A stubborn raw material: The conversion of cellulosic biomass into low-price biofuels and high-value-added chemicals is a very challenging goal. This Review addresses the development of the enzymatic catalytic degradation of (ligno)cellulose (see picture), including achievements in the areas of chemical-reaction engineering, structural biochemistry, and catalyst design.

Communications

Mössbauer Spectroscopy

H. Peng, S. Tricard, G. Félix, G. Molnár,
W. Nicolazzi, L. Salmon,*
A. Bousseksou* ________ 10894 – 10898

Re-Appearance of Cooperativity in Ultra-Small Spin-Crossover [Fe(pz){Ni(CN)$_4$}] Nanoparticles

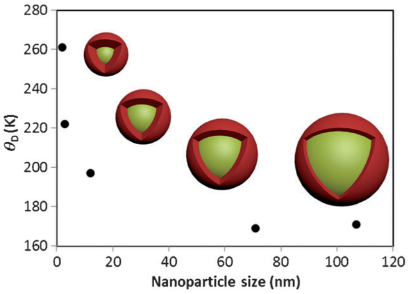

Spin-crossover nanoparticles: Mössbauer spectroscopy was used to determine the variation of the Debye temperature (θ_D) for [Fe(pz){Ni(CN)$_4$}] (py = pyrazine) spin-crossover nanoparticles ranging from 2 to 110 nm (see picture). The investigations explain the re-appearance of cooperativity in the smallest nanoparticles.

Frontispiece

Dendrimers

S. Zhang, R.-O. Moussodia, H.-J. Sun,
P. Leowanawat, A. Muncan,
C. D. Nusbaum, K. M. Chelling,
P. A. Heiney, M. L. Klein, S. André, R. Roy,
H.-J. Gabius, V. Percec* ___ **10899 – 10903**

Mimicking Biological Membranes with Programmable Glycan Ligands Self-Assembled from Amphiphilic Janus Glycodendrimers

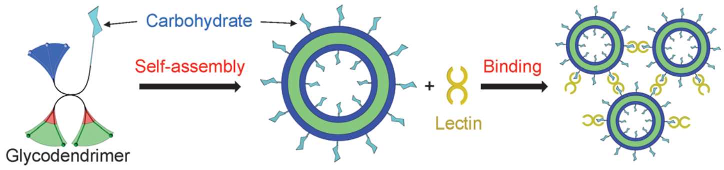

Glycodendrimersomes: Amphiphilic Janus glycodendrimers with different topologies self-assemble into uniform unilamellar soft vesicles, denoted glycodendrimersomes, which are stable over time. They exhibit specific and potent bioactivity in binding biomedically relevant lectins. The vesicles with multivalent glycan ligands extending beyond their surface were shown to provide optimal glycan ligand display.

Protein Design

R. M. Hughes,
D. S. Lawrence* ___ **10904 – 10907**

Optogenetic Engineering: Light-Directed Cell Motility

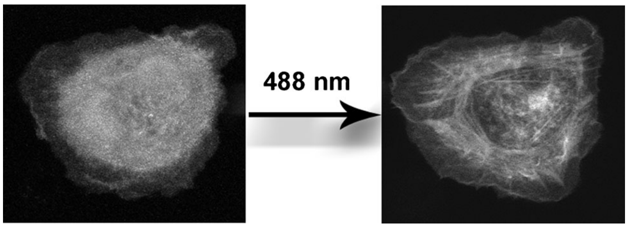

Shine a light: A straightforward strategy for the acquisition of genetically encoded, light-activatable proteins is based upon the principles set forth in the 100 year old Michaelis–Menten Equation. Photoactivation of a light-responsive cofilin mediates cytoskeleton remodelling, lamellipodia and filopodia formation, and directed cell motility.

Luminescence

M. Han, Y. Tian, Z. Yuan, L. Zhu,
B. Ma* ___ **10908 – 10912**

A Phosphorescent Molecular “Butterfly” that undergoes a Photoinduced Structural Change allowing Temperature Sensing and White Emission

The white brothers: A molecular “butterfly”, that is, a phosphorescent Pt^{II} binuclear complex, can flap its “wings” and generate dual (white) emission upon photoexcitation. This photoinduced molecular structure change results from the shortening of the Pt–Pt distance in the excited state and is phase-dependent allowing application of the complex as a self-referenced luminescent sensor for phase change, temperature, and viscosity.

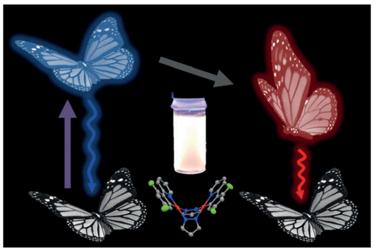

Methylidene Complexes

M. Kamitani, B. Pinter, C. H. Chen,
M. Pink, D. J. Mindiola* ___ **10913 – 10915**

Mononuclear and Terminal Zirconium and Hafnium Methylidenes

Front Cover

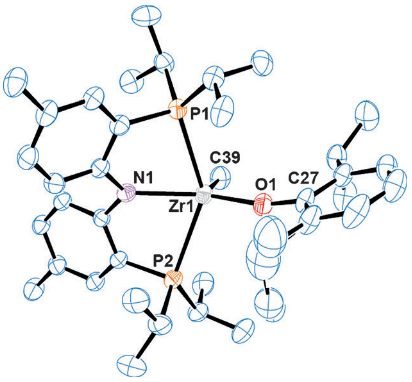

The photolysis of zirconium or hafnium complexes with one aryloxide and two methyl ligands induces α-hydrogen abstraction and results in the formation of mononuclear complexes with terminal methylidene ligands. These unique systems have been fully characterized, including the determination of the solid-state structure in the case of the zirconium complex.

Analytical Methods

Q. Q. Wan, S. M. Chen, W. Shi, L. H. Li, H. M. Ma* **10916 – 10920**

Lysosomal pH Rise during Heat Shock Monitored by a Lysosome-Targeting Near-Infrared Ratiometric Fluorescent Probe

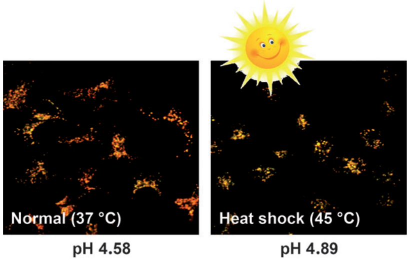

Feeling hot, hot, hot: A near-infrared ratiometric pH probe with a stable semicyanine skeleton has been developed for lysosomal pH measurements. The readily preparable probe shows an excellent lysosome-targeting ability and high photostability. The probe has been used to investigate the change of lysosomal pH with temperature, revealing for the first time that lysosomal pH values rise during heat shock and the process is irreversible.

Bioorthogonal Chemistry

S. Letschert, A. Göhler, C. Franke, N. Bertleff-Zieschang, E. Memmel, S. Doose,* J. Seibel,* M. Sauer* **10921 – 10924**

Super-Resolution Imaging of Plasma Membrane Glycans

Glycan spotting: Click chemistry and super-resolution imaging was used to visualize and quantify ManNAc-, GalNAc-, and O-GlcNAc-modified glycans in the plasma membrane of mammalian cells with single-molecule sensitivity (see image). The data demonstrate that a single cell may easily contain more than ten million glycans, which are homogeneously distributed and do not form clusters or nanodomains.

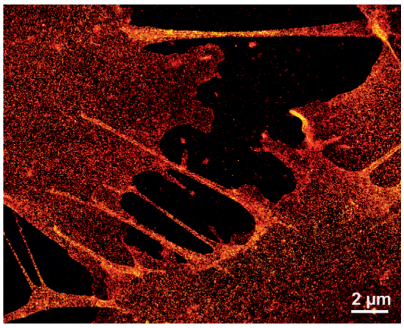

Biocatalysis

A. M. Rydzik, I. K. H. Leung, G. T. Kochan, M. A. McDonough, T. D. W. Claridge, C. J. Schofield* **10925 – 10927**

Oxygenase-Catalyzed Desymmetrization of *N*,*N*-Dialkyl-piperidine-4-carboxylic Acids

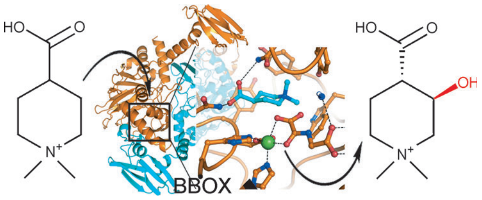

Thinking outside the BBOX: γ-Butyrobetaine hydroxylase (BBOX) is a 2-oxoglutarate (2OG) dependent oxygenase that catalyzes the final hydroxylation step in the biosynthesis of carnitine. BBOX was shown to catalyze the oxidative desymmetrization of achiral *N*,*N*-dialkyl-piperidine-4-carboxylates to give products with two or three stereogenic centers.

Bioconjugation

P. Schmidt, L. Zhou, K. Tishinov, K. Zimmermann, D. Gillingham* **10928 – 10931**

Dialdehydes Lead to Exceptionally Fast Bioconjugations at Neutral pH by Virtue of a Cyclic Intermediate

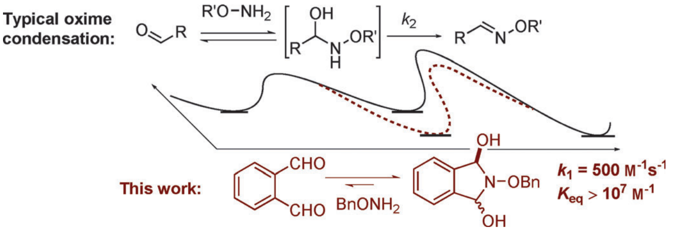

For aldehydes, 1 + 1 = 500: Dialdehydes react with *O*-alkylhydroxylamines at rates of 500 $\text{M}^{-1}\,\text{s}^{-1}$ at neutral pH values in the absence of catalysts. The key to these conjugations is an unusually stable cyclic intermediate, which ultimately undergoes dehydration to yield an oxime. The application of this method in bioconjugations and a mechanistic interpretation are outlined.

Copolymerization

H. Aoshima, M. Uchiyama, K. Satoh,*
M. Kamigaito* ________ **10932 – 10936**

Interconvertible Living Radical and Cationic Polymerization through Reversible Activation of Dormant Species with Dual Activity

Inside Cover

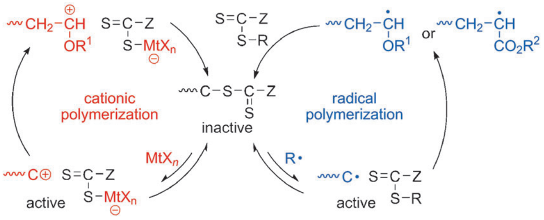

Dr. Jekyll and Mr. Hyde: A dormant thioester bond with dual activity is reversibly activated by radicals and Lewis acids to induce concurrent radical and cationic polymerizations. This method enables the controlled synthesis of multiblock copolymers comprised of different types of segments that cannot be prepared with a single intermediate.

Collective Tunneling

C. Drechsel-Grau,*
D. Marx* ____________ **10937 – 10940**

Exceptional Isotopic-Substitution Effect: Breakdown of Collective Proton Tunneling in Hexagonal Ice due to Partial Deuteration

Ab initio simulations clarify the effects of H/D isotopic substitution on the mechanism of the collective tunneling of six protons within proton-ordered cyclic water hexamers that are contained in proton-disordered ice. At the transition state, isotopic substitution leads to a Zundel-like [HO···D···OH] complex with localized ionic defects and thus inhibits perfectly correlated proton tunneling.

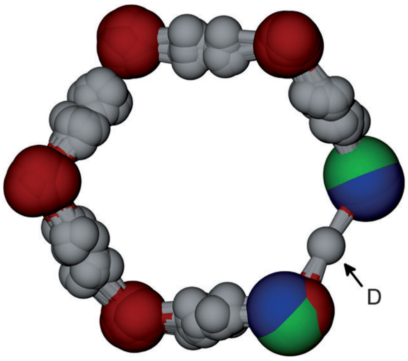

Conformational Space

T. Yamaguchi, Y. Sakae, Y. Zhang,
S. Yamamoto, Y. Okamoto,
K. Kato* ____________ **10941 – 10944**

Exploration of Conformational Spaces of High-Mannose-Type Oligosaccharides by an NMR-Validated Simulation

Watch this space: Lanthanide- and isotope-assisted NMR approaches combined with replica-exchange molecular dynamics simulations have been used to describe the conformational dynamics of complicated, branched oligosaccharides. The experimentally validated simulation provided quantitative views of the dynamic conformational ensembles of oligosaccharides with triantennary structures.

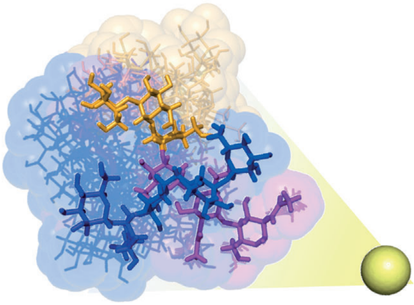

Drug Delivery

W. J. Smith, N. P. Oien, R. M. Hughes,
C. M. Marvin, Z. L. Rodgers, J. Lee,
D. S. Lawrence* ________ **10945 – 10948**

Cell-Mediated Assembly of Phototherapeutics

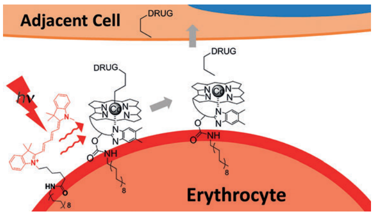

Window of opportunity: A wavelength-encoded drug-delivery strategy operates within the optical window of tissue. The photoresponsive system is acquired by the assembly of lipid-cobalamin-drug and lipid-fluorophore constructs on the surface of erythrocytes. The desired wavelength of cobalamin-drug photocleavage is “dialed-in” by simply choosing the appropriate lipid-fluorophore “antenna”.

Controlled Drug Delivery

Z. Zhou, X. Ma, C. J. Murphy, E. Jin,
Q. Sun, Y. Shen,* E. A. Van Kirk,
W. J. Murdoch ——— 10949 – 10955

Molecularly Precise Dendrimer–Drug Conjugates with Tunable Drug Release for Cancer Therapy

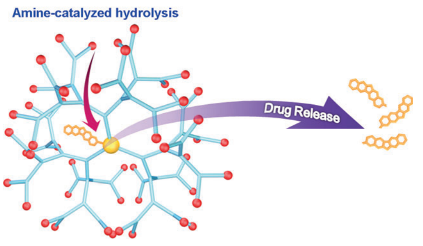

Camptothecine core: Polylysine dendrimers with the conjugated drug in the core were synthesized for cancer therapy. The release rates of the camptothecine conjugates were easily tunable by adjusting the dendrimer generation and the peripheral functional groups as well as the pH. Conjugates showing a fast drug release also exhibited a high anticancer activity against intraperitoneal and subcutaneous tumors.

RNA Targeting

S. G. Rzuczek, H. Park,
M. D. Disney* ——— 10956 – 10959

A Toxic RNA Catalyzes the In Cellulo Synthesis of Its Own Inhibitor

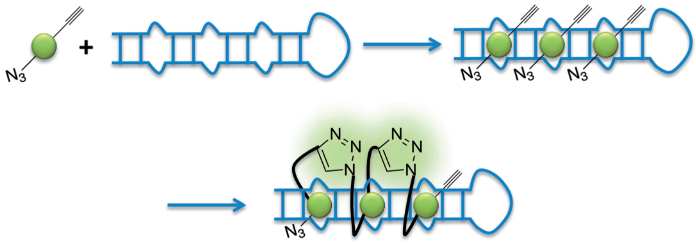

Potent modulators of RNA function can be assembled in cellulo by using the cell as the reaction vessel and a disease-causing RNA as the catalyst. In particular, a Huisgen 1,3-dipolar cycloaddition reaction was used to template the synthesis of an RNA inhibitor in disease-affected cells.

Oxygen Evolution

K. Sardar, E. Petrucco, C. I. Hiley,
J. D. B. Sharman, P. P. Wells,
A. E. Russell,* R. J. Kashtiban, J. Sloan,
R. I. Walton* ——— 10960 – 10964

Water-Splitting Electrocatalysis in Acid Conditions Using Ruthenate-Iridate Pyrochlores

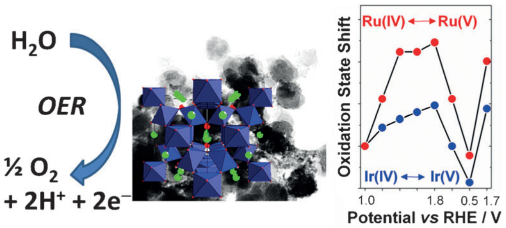

Ru/Ir cooperativity: A pyrochlore solid solution $(Na_{0.33}Ce_{0.67})_2(Ir_{1-x}Ru_x)_2O_7$ formed as nanocrystalline powder under hydrothermal conditions shows high activity for electrochemical oxygen evolution in aqueous acid. In situ XAFS experiments show a cooperative effect of Ru and Ir that depends on the composition of the material. OER = oxygen evolution reaction.

Metal–Organic Supercontainers

N. L. Netzer, F. R. Dai, Z. Wang,*
C. Jiang* ——— 10965 – 10969

pH-Modulated Molecular Assemblies and Surface Properties of Metal–Organic Supercontainers at the Air–Water Interface

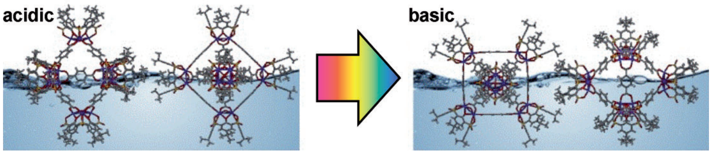

MOSC thin films: The molecular assemblies of metal–organic supercontainers (MOSCs) were studied at the air–water interface. Variation in the pH values of the subphases causes significant changes in the molecular orientation in the Langmuir films. The uniform MOSC structures in Langmuir–Blodgett films show tunable surface properties that can be precisely controlled by the fabricating conditions.

Natural Products

Cascades: The total synthesis of the cytotoxic myceliothermophins C, D, and E have been achieved through a sequence involving a cascade bis(cyclization) of epoxide or aldehyde substrates to forge a *trans*-fused decalin precursor of the natural products.

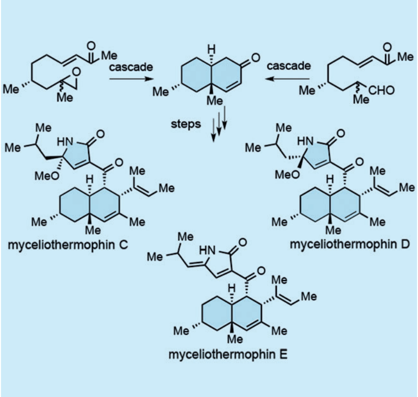

Receptor Targeting

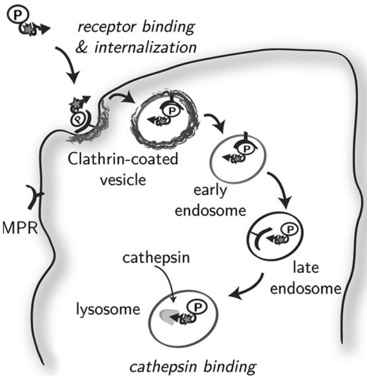

On target: A synthetic glycopeptide (P) that contains six mannose-6-phosphate residues was covalently attached to a fluorescent activity-based probe for cathepsins. The construct was internalized in live cells through binding to the mannose-6-phosphate receptor (MPR), thus validating the cluster as an MPR-targeting ligand that can be used to deliver cargo into the endolysosomal pathway.

Gas-Phase Reactions

Inside Back Cover

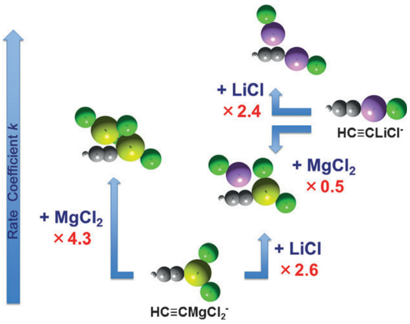

How do individual salt molecules influence the kinetic basicity of organometallates reacting with water? Addition of LiCl to $[HCCLiCl]^-$ or $[HCCMgCl_2]^-$ enhances their reactivity towards water by a factor of about two, while addition of $MgCl_2$ to $[HCCMgCl_2]^-$ enhances its reactivity by a factor of about four (see picture). The mechanism of hydration has been studied theoretically.

Radicals

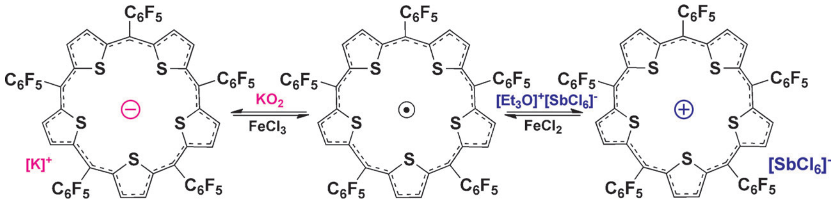

Super stable: A 25π radical of an expanded isophlorin undergoes reversible one-electron oxidation to form 24π antiaromatic species and one-electron reduction to form 26π aromatic species, confirming its amphoteric behavior. All of the three oxidation states of the macrocycle have been characterized in solution and the solid state to confirm their stability under ambient conditions.

Flavin Redox Bifurcation

A. Okamoto,* K. Hashimoto, K. H. Nealson* ________ 10988 – 10991

Flavin Redox Bifurcation as a Mechanism for Controlling the Direction of Electron Flow during Extracellular Electron Transfer

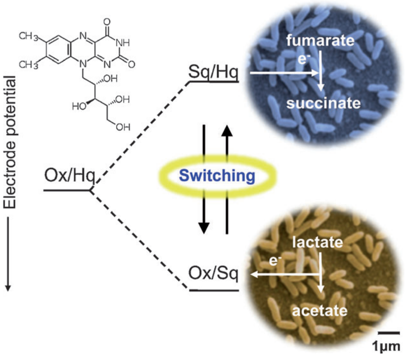

The iron-reducing bacterium *Shewanella oneidensis* MR-1 has a dual directional electronic conduit involving 40 heme redox centers in flavin-binding outer-membrane *c*-type cytochromes (OM *c*-Cyts). The redox bifurcation of the cell-secreted riboflavin cofactor in OM *c*-Cyts switches the direction of electron conduction in the biological conduit at the cell–electrode interface to drive either bacterial electrode reduction or oxidation reactions. Sq = semiquinone, Hq = hydroquinone.

Synthetic Methods

J. L.-Y. Chen, V. K. Aggarwal* ________ 10992 – 10996

Highly Diastereoselective and Enantiospecific Allylation of Ketones and Imines Using Borinic Esters: Contiguous Quaternary Stereogenic Centers

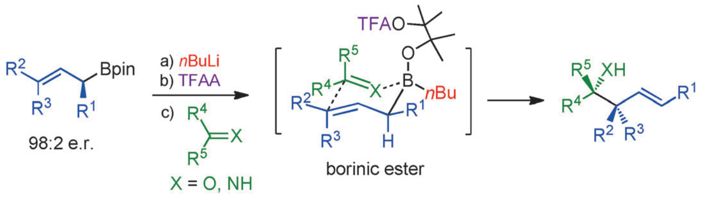

Goldilocks reactivity: 3,3-Disubstituted allylic borinic esters possess the perfect balance between reactivity and configurational stability to react with both ketones and ketimines, allowing facile access to adjacent quaternary stereocenters with full stereocontrol. Synthesis of all possible stereoisomers of a quaternary-quaternary motif is demonstrated. TFAA = trifluoroacetic anhydride.

Synthetic Methods

C. Nagaraju, K. R. Prasad* ________ 10997 – 11000

An Unusual Ring-Contraction/Rearrangement Sequence for Making Functionalized Di- and Triquinanes

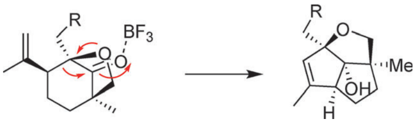

In sync: An unusual rearrangement involving a ring contraction and subsequent intramolecular trapping of the incipient oxocarbenium ion with an alkene has been observed. The rearrangement offers a new route to structurally complex diquinanes (see scheme). The sequence was extended to the synthesis of an oxymethano-bridged triquinane framework.

Photocatalysis

M. K. Bhunia, K. Yamauchi, K. Takanabe* ________ 11001 – 11005

Harvesting Solar Light with Crystalline Carbon Nitrides for Efficient Photocatalytic Hydrogen Evolution

Back Cover

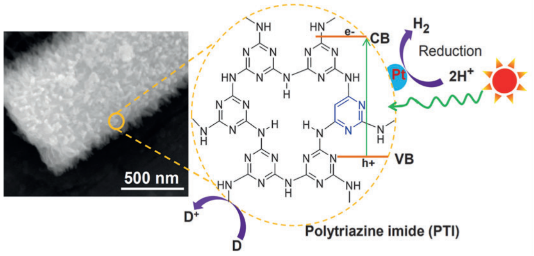

Trying out triazine: Crystalline carbon nitrides have been synthesized by employing supramolecular aggregation and ionic melt polycondensation. The triazine-based carbon nitride exhibits the excellent hydrogen evolution reaction rate at visible light and apparent quantum yield reaches about 7 % at 420 nm.

Dinuclear Metal Complexes

R. D. Adams,* V. Rassolov,*
Y. O. Wong ______ 11006 – 11009

Facile C—H Bond Formation by Reductive Elimination at a Dinuclear Metal Site

The electronically unsaturated dirhenium complex $[Re_2(CO)_8(\mu\text{-}AuPPh_3)(\mu\text{-}Ph)]$ was obtained from the reaction of $[Re_2(CO)_8\{\mu\text{-}\eta^2\text{-}C(H){=}C(H)n\text{Bu}\}(\mu\text{-}H)]$ with $[Au(PPh_3)Ph]$, and by reaction with $HSnPh_3$ was converted into $[Re_2(CO)_8(\mu\text{-}H)(\mu\text{-}Ph)]$ (see picture). This hydrido-bridged complex reductively eliminates benzene upon addition of NCMe.

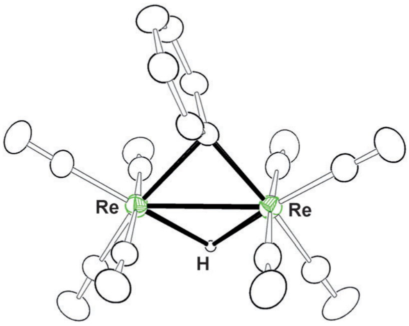

CO_2 Utilization

K. Beydoun, G. Ghattas, K. Thenert,
J. Klankermayer,*
W. Leitner ______ 11010 – 11014

Ruthenium-Catalyzed Reductive Methylation of Imines Using Carbon Dioxide and Molecular Hydrogen

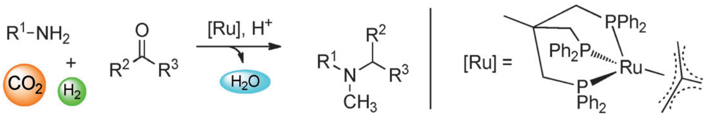

Tertiary *N*-methylamines were obtained in good to excellent yields through the reductive methylation of imines (used as such or formed in situ from amines and aldehydes, see scheme). Apart from the well-defined [Ru(triphos)(tmm)] catalyst, CO_2 was used as the C_1 source, and H_2 as the reducing agent. This method enabled the preparation of the antifungal agent butenafine in one step with no apparent waste, thus increasing the atom efficiency of its synthesis.

Microwave Spectroscopy

C. Bermúdez, S. Mata, C. Cabezas,
J. L. Alonso* ______ 11015 – 11018

Tautomerism in Neutral Histidine

Conformational analysis: Neutral histidine has been generated in the gas phase by laser ablation of solid samples, and its $N_\varepsilon H$ tautomeric form has been unraveled through its rotational spectrum (see picture). The quadrupole hyperfine structure, arising from the existing three ^{14}N nuclei, constituted a site-specific probe for revealing the tautomeric form as well as the side-chain configuration of this proteogenic amino acid.

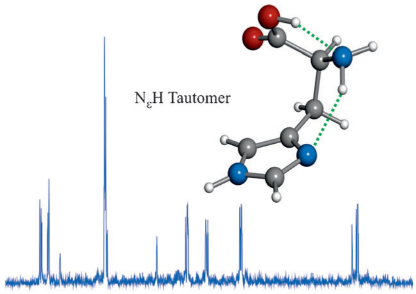

Natural Products

R. Teufel, L. Kaysser, M. T. Villaume,
S. Diethelm, M. K. Carbullido, P. S. Baran,
B. S. Moore* ______ 11019 – 11022

One-Pot Enzymatic Synthesis of Merochlorin A and B

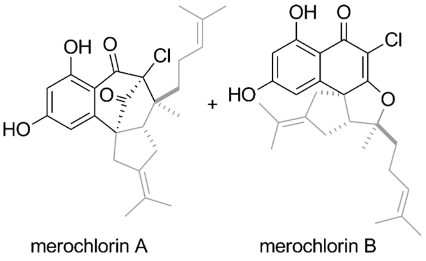

Assembly line: The biosynthetic pathway to merochlorins A and B was fully reconstituted in vitro and involves only four enzymes. The assembly route starts from the common metabolites dimethylallyl diphosphate, geranyl diphosphate, and malonyl CoA, which are transformed into an unusual polyketide-terpene hybrid intermediate. Oxidative chlorination and terpene cyclization complete the remarkably short pathway to the merochlorins.

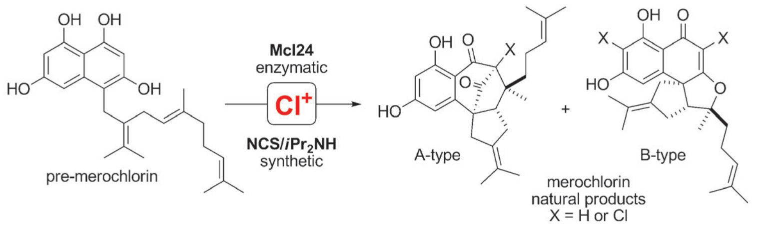

Naturally inspiring: The vanadium-dependent chloroperoxidase Mcl24 was found to mediate a complex series of transformations in the biosynthesis of the merochlorins, in particular, a site-selective naphthol chlorination and an oxidative dearomatization/terpene cyclization sequence to build up the stereochemically complex carbon framework. Inspired by the enzyme reactivity, a chemical chlorination procedure paralleling the biocatalytic process was developed.

Natural Product Synthesis

S. Diethelm, R. Teufel, L. Kaysser,
B. S. Moore* ________ **11023 – 11026**

A Multitasking Vanadium-Dependent Chloroperoxidase as an Inspiration for the Chemical Synthesis of the Merochlorins

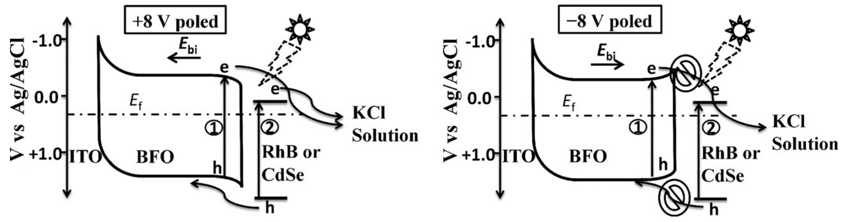

Poling station: The orientation of the $BiFeO_3$ (BFO) band bending at the BFO/electrolyte in polycrystalline BFO photoelectrodes can be switched from upwards to downwards by poling pretreatments of +8 V or −8 V, respectively. It is thus possible to manipulate photoelectrochemical reactions on a single ferroelectric photoelectrode.

Photoelectrodes

D. Cao, Z. Wang, Nasori, L. Wen, Y. Mi,
Y. Lei* ________ **11027 – 11031**

Switchable Charge-Transfer in the Photoelectrochemical Energy-Conversion Process of Ferroelectric $BiFeO_3$ Photoelectrodes

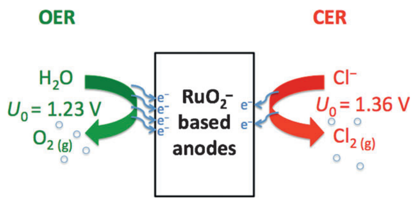

Being selective: The selectivity in the industrially important Chlor-Alkali process has been elucidated on the microscopic level through a combination of DFT calculations and volcano plots. A single layer of TiO_2(110) grown on RuO_2(110) increases the selectivity between the chlorine and oxygen evolution reactions (CER and OER, respectively) by several orders of magnitude, while keeping the high activity for CER practically constant.

Electrocatalysis

K. S. Exner, J. Anton, T. Jacob,
H. Over* ________ **11032 – 11035**

Controlling Selectivity in the Chlorine Evolution Reaction over RuO_2-Based Catalysts

The redox couple ferrocene/ferrocenium has been applied for the construction of a liquid cathode Li-ion redox battery for electrical energy storage. The redox reaction is highly reversible and efficient. Even after 250 full charge/discharge cycles the capacity maintains about 90 % of the initial value and the Coulombic efficiency reaches 98–100 %.

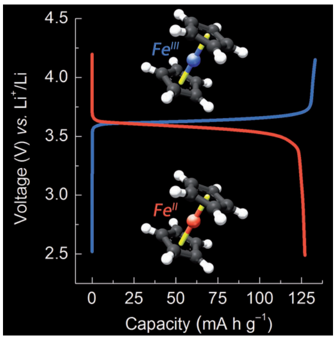

Li-Ion Batteries

VIP

Y. Zhao, Y. Ding, J. Song, G. Li, G. Dong,
J. B. Goodenough, G. Yu* **11036 – 11040**

Sustainable Electrical Energy Storage through the Ferrocene/Ferrocenium Redox Reaction in Aprotic Electrolyte

Asymmetric Catalysis

S. Lu, S. B. Poh, Y. Zhao* **11041 – 11045**

Kinetic Resolution of 1,1′-Biaryl-2,2′-Diols and Amino Alcohols through NHC-Catalyzed Atroposelective Acylation

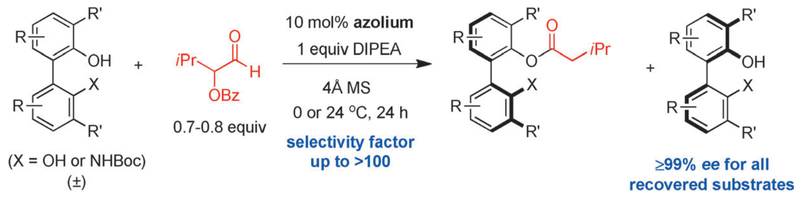

BINOL and NOBIN derivatives can be obtained in high enantioselectivities of ≥ 99 % *ee* through NHC-catalyzed kinetic resolution. This method presents the first highly enantioselective catalytic acylation of axially chiral alcohols.

Isotopic Labeling

D. van der Born, C. Sewing, J. D. M. Herscheid, A. D. Windhorst, R. V. A. Orru, D. J. Vugts* **11046 – 11050**

A Universal Procedure for the [^{18}F]Trifluoromethylation of Aryl Iodides and Aryl Boronic Acids with Highly Improved Specific Activity

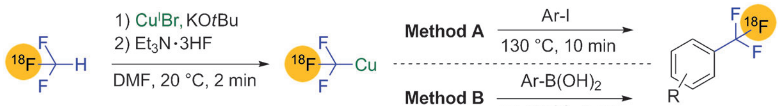

A quality label: Tracers for positron emission tomography (PET) with a [^{18}F]CF$_3$ group directly attached to an arene were synthesized with improved specific activity by the trifluoromethylation of aryl iodides and aryl boronic acids with [^{18}F]trifluoromethane (see scheme). In particular, the trifluoromethylation of aryl boronic acids proceeded rapidly under mild reaction conditions, thus making this method highly suitable for the production of PET tracers.

Heterocycle Synthesis

G. Mei, H. Yuan, Y. Gu, W. Chen, L. W. Chung, C.-C. Li* **11051 – 11055**

Dearomative Indole [5+2] Cycloaddition Reactions: Stereoselective Synthesis of Highly Functionalized Cyclohepta[*b*]indoles

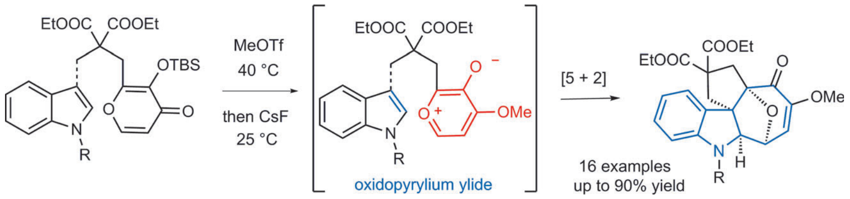

Bridge construction: The title reaction with an oxidopyrylium ylide resulted in efficient and diastereoselective construction of highly functionalized oxacyclohepta[*b*]indoles. The procedure proceeded under very mild reaction conditions, thus enabling high functional-group tolerance and *endo* selectivity. TBS = *tert*-butyldimethylsilyl, Tf = trifluoromethanesulfonyl.

Photocatalysis

T. R. Blum, Y. Zhu, S. A. Nordeen, T. P. Yoon* **11056 – 11059**

Photocatalytic Synthesis of Dihydrobenzofurans by Oxidative [3+2] Cycloaddition of Phenols

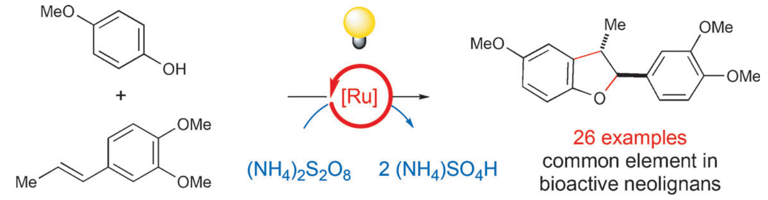

In a good light: The versatile photoredox properties of Ru^{II} chromophores offer a strategy to couple powerful oxidative transformations to benign inorganic peroxysulfate oxidants. In this example, the photocatalytic [3+2] cycloaddition of phenols and electron-rich styrenes for the synthesis of diverse dihydrobenzofurans is presented.

Photochemistry

S. A. Moteki, A. Usui, S. Selvakumar, T. Zhang, K. Maruoka* ___ 11060 – 11064

Metal-Free C−H Bond Activation of Branched Aldehydes with a Hypervalent Iodine(III) Catalyst under Visible-Light Photolysis: Successful Trapping with Electron-Deficient Olefins

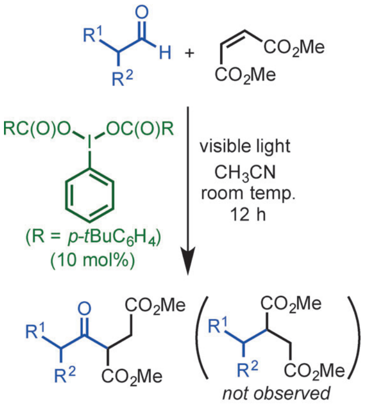

A radical approach: The mild photocatalyzed activation of the C(O)−H bond in branched aldehydes offers easy access to acyl radicals and, without decarbonylation, allowed the efficient synthesis of unsymmetrical ketones by trapping with electrophilic olefins. A characteristic feature of this approach is the catalytic use of a hypervalent iodine(III) reagent to generate radicals.

ortho Alkylation

B. M. Monks, E. R. Fruchey, S. P. Cook* ___ 11065 – 11069

Iron-Catalyzed C(sp^2)−H Alkylation of Carboxamides with Primary Electrophiles

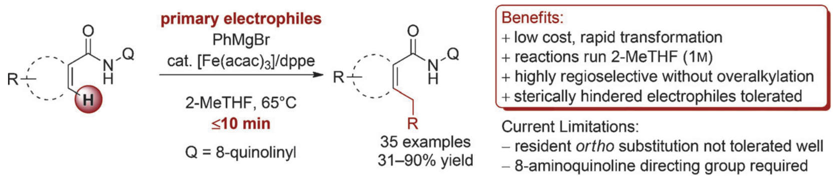

The direct *ortho* alkylation of 8-aminoquinoline-based aryl amides was achieved with primary alkyl bromides in high yields in the presence of an iron catalyst, 1,2-bis(diphenylphosphino)ethane (dppe), and PhMgBr in 2-MeTHF.

Cross-Coupling

D. Zhang, G. Xu, D. Ding, C. Zhu, J. Li, J. Sun* ___ 11070 – 11074

Gold(I)-Catalyzed Diazo Coupling: Strategy towards Alkene Formation and Tandem Benzannulation

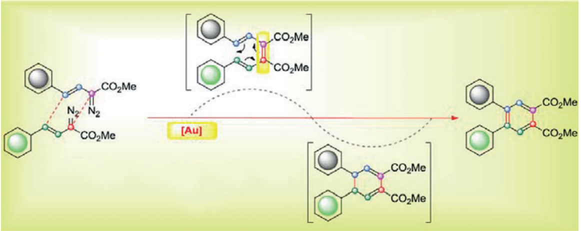

Crossing paths: A gold(I)-catalyzed cross-coupling of diazo compounds to afford tetrasubstituted alkenes has been developed. In addition, a gold(I)-initiated benzannulation has been achieved in a tandem reaction involving cross-coupling of the vinyldiazoacetates, sequential 6π electrocyclization, and oxidative aromatization.

Natural Product Synthesis

X. Han, P. E. Floreancig* 11075 – 11078

Spiroacetal Formation through Telescoped Cycloaddition and Carbon–Hydrogen Bond Functionalization: Total Synthesis of Bistramide A

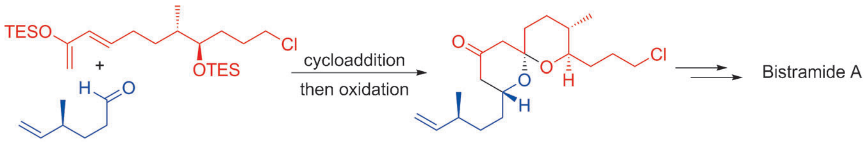

Actin' out: Spiroacetals can be prepared from aldehydes and functionalized dienes through a convergent, telescoped sequence of cycloaddition, oxidative C−H bond cleavage, and acid treatment. The functional-group tolerance and facile accessibility of the components render this procedure suitable for the synthesis of structurally complex natural products such as the actin-binding cytotoxin bistramide A.

Sythetic Methods

H.-W. Zhang, Y. C. Song, J. B. Zhao,
J. P. Zhang,* Q. Zhang* **11079–11083**

Regioselective Radical Aminofluorination of Styrenes

Double agent: The copper-catalyzed radical aminofluorination of styrenes with *N*-fluorobenzenesulfonimide (NFSI) has been realized with high regioselectivity, thus affording aminofluorination products with regioselectivities opposite to those of the palladium-catalyzed and noncatalyzed processes. NFSI reacts under N–F bond homolysis and is utilized as both a radical nitrogen source and radical fluorine source.

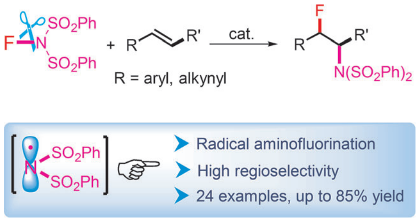

Cyclization

X. Wang, J. Gallardo-Donaire,
R. Martin* **11084–11087**

Mild ArI-Catalyzed C(sp^2)–H or C(sp^3)–H Functionalization/C–O Formation: An Intriguing Catalyst-Controlled Selectivity Switch

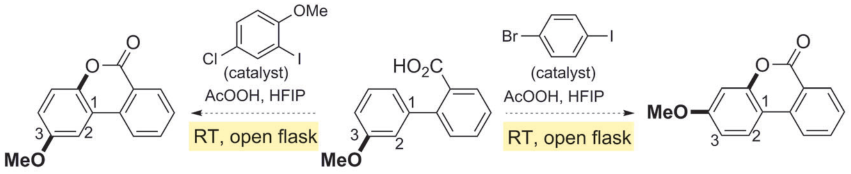

Who controls the switch? I! A tandem C(sp^2)–H or C(sp^3)–H functionalization/C–O bond-forming reaction catalyzed by I^{III} reagents generated in situ has been developed. The transformation shows broad scope under mild conditions and exhibits an unprecedented selectivity profile that can be switched depending on the nature of the iodine catalyst employed (see scheme; HFIP = 1,1,1,3,3,3-hexafluoro-2-propanol).

Cross-Coupling

H. Cai, K. Fujimoto, J. M. Lim, C. Wang,
W. Huang, Y. Rao, S. Zhang, H. Shi, B. Yin,
B. Chen, M. Ma, J. Song,* D. Kim,*
A. Osuka* **11088–11091**

Synthesis of Direct β-to-β Linked Porphyrin Arrays with Large Electronic Interactions: Branched and Cyclic Oligomers

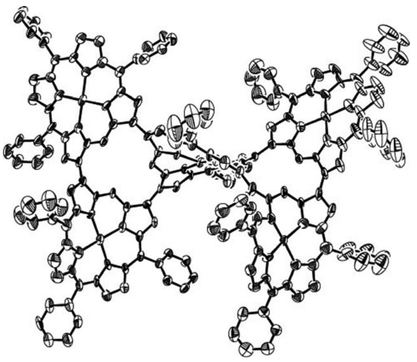

Molecular twine: The title porphyrin trimers and pentamers have been synthesized by Suzuki–Miyaura coupling of β-boryl-porphyrins and β-bromoporphyrins. The cyclic porphyrin trimer, the smallest directly linked cyclic porphyrin, and its twined pentamer exhibit small HOMO–LUMO gaps, broad nonsplit Soret bands, red-shifted Q-bands, and efficient excitation-energy hopping.

Ruthenium Pincer Complexes

D. Srimani, G. Leitus, Y. Ben-David,
D. Milstein* **11092–11095**

Direct Catalytic Olefination of Alcohols with Sulfones

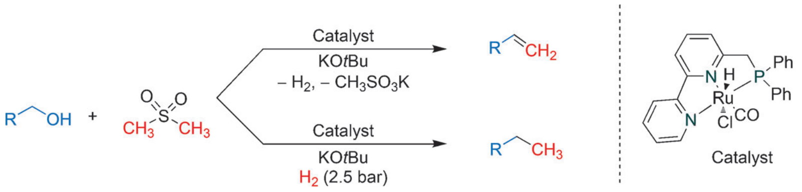

The one-step olefination of alcohols with sulfones for the direct synthesis of terminal and internal olefins can be catalyzed by ruthenium pincer complexes. Furthermore, performing the reaction with dimethyl sulfone under mild hydrogen pressure provides a one-step method for the replacement of alcohol hydroxy groups by methyl groups.

Supporting information is available on www.angewandte.org (see article for access details).

A video clip is available as Supporting Information on www.angewandte.org (see article for access details).

This article is available online free of charge (Open Access).

This article is accompanied by a cover picture (front or back cover, and inside or outside).

The Very Important Papers, marked VIP, have been rated unanimously as very important by the referees.

The Hot Papers are articles that the Editors have chosen on the basis of the referee reports to be of particular importance for an intensely studied area of research.

Angewandte Corrigendum

The footnotes in Tables 1 and 2 of this communication were labeled incorrectly. The footnote for ECA yield should be changed to [c] (previously [d]) and the footnote corresponding to e.r. values should be changed to [d] (previously [e]). All yields are of isolated and purified products. In Table 1, entries 7 and 8 correspond to the only reactions for which catalyst **1c** was used. In Table 2, only entries 11 and 12 relate to transformations where catalyst precursor **1a** was utilized. The accurate versions of Tables 1 and 2 are provided below. The Supporting Information has been amended as well.

A Multicomponent Ni-, Zr-, and Cu-Catalyzed Strategy for Enantioselective Synthesis of Alkenyl-Substituted Quaternary Carbons

K. P. McGrath,
A. H. Hoveyda* ________ **1910–1914**

Angew. Chem. Int. Ed. **2014**, *53*

DOI: 10.1002/anie.201309456

Table 1: Multicomponent catalytic reactions with β-alkenylaluminum reagents.[a]

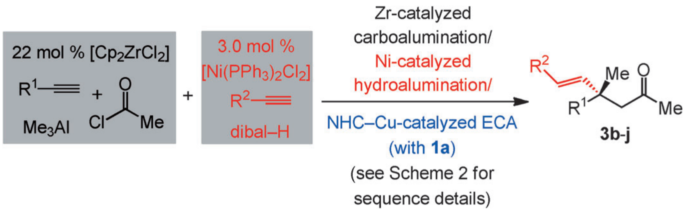

Entry	R^1; R^2	ECA conv. [%][b]	Prod.	Carbomet./acyl. yield [%];[c] ECA yield [%][c]	e.r.[d]
1	*p*MeOC$_6$H$_4$; C$_6$H$_5$	> 98	**3b**	40; 75	98:2
2	*p*BrC$_6$H$_4$; C$_6$H$_5$	> 98	**3c**	63; 60	96:4
3	C$_6$H$_5$; *p*MeOC$_6$H$_4$	> 98	**3d**	80; 60	96.5:3.5
4	C$_6$H$_5$; *p*F$_3$CC$_6$H$_4$	> 98	**3e**	80; 72	98:2
5	*o*MeOC$_6$H$_4$; C$_6$H$_5$	> 98	**3f**	80; 60	98:2
6	C$_6$H$_5$; 3-thienyl	> 98	**3g**	80; 54	96.5:3.5
7	Cy; C$_6$H$_5$[e]	> 98	**3h**	61; 51	97:3
8	CH$_2$C$_6$H$_5$; C$_6$H$_5$[e]	> 98	**3i**	80; 55	90.5:9.5
9	C$_6$H$_5$; Cy	> 98	**3j**	80; 60	94.5:5.5

[a] Reactions were performed under N$_2$ atmosphere; enones generated with > 98 % *E* selectivity in all cases. [b] Determined by analysis of 400 MHz ^{1}H NMR spectra of unpurified mixtures (± 2 %). [c] Yield of isolated and purified products (± 5 %). [d] Determined by HPLC analysis; see the Supporting Information for details. [e] NHC-Ag complex **1c** was used as catalyst precursor.

Table 2: Multicomponent catalytic reactions with α-alkenylaluminum reagents.[a]

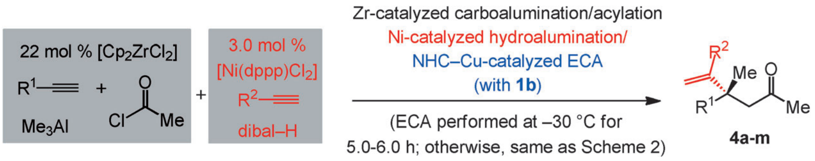

Entry	R^1; R^2	ECA conv. [%][b]	Prod.	Carbomet./acyl. yield [%];[c] ECA yield [%][c]	e.r.[d]
1	C$_6$H$_5$; C$_6$H$_5$	> 98	**4a**	80; 82	99:1
2	*p*MeOC$_6$H$_4$; C$_6$H$_5$	> 98	**4b**	40; 95	97.5:2.5
3	*m*FC$_6$H$_4$; C$_6$H$_5$	> 98	**4c**	88; 88	99:1
4	*o*FC$_6$H$_4$; C$_6$H$_5$	88	**4d**	60; 48	99:1
5	C$_6$H$_5$; *p*MeOC$_6$H$_4$	> 98	**4e**	80; 95	98:2
6	C$_6$H$_5$; *p*F$_3$CC$_6$H$_4$	> 98	**4f**	80; 80	97:3
7	C$_6$H$_5$; *m*F$_3$CC$_6$H$_4$	> 98	**4g**	80; 97	98:2
8	C$_6$H$_5$; *o*FC$_6$H$_4$	> 98	**4h**	80; 71	99:1
9	*p*MeOC$_6$H$_4$; 3-thienyl	> 98	**4i**	40; 81	98:2
10	*p*BrC$_6$H$_4$; C$_6$H$_5$	> 98	**4j**	63; 95	99:1
11	(CH$_2$)$_3$OTBS; C$_6$H$_5$[e]	> 98	**4k**	62; 87	95:5
12	CH$_2$C$_6$H$_5$; C$_6$H$_5$[e]	> 98	**4l**	80; 85	97.5:2.5
13	Cy; C$_6$H$_5$	> 98	**4m**	61; 83	92:8

[a] Reactions were performed under N$_2$ atmosphere; enones generated with > 98 % *E* selectivity in all cases. [b] Determined by analysis of 400 MHz ^{1}H NMR spectra of unpurified mixtures (± 2 %). [c] Yield of isolated and purified products (± 5 %). [d] Determined by HPLC analysis; see the Supporting Information for details. [e] NHC-Ag complex **1a** was used as catalyst precursor.